

# A Simple Model with Myofilament Compliance Predicts Activation-Dependent Crossbridge Kinetics in Skinned Skeletal Fibers

D. A. Martyn,\* P. B. Chase,<sup>†</sup> M. Regnier,\* and A. M. Gordon<sup>‡</sup>

Departments of \*Bioengineering and <sup>†</sup>Physiology and Biophysics, University of Washington, Seattle, Washington 98195, and <sup>‡</sup>Department of Biological Sciences, Florida State University, Tallahassee, Florida 32306 USA

**ABSTRACT** The contribution of thick and thin filaments to skeletal muscle fiber compliance has been shown to be significant. If similar to the compliance of cycling cross-bridges, myofilament compliance could explain the difference in time course of stiffness and force during the rise of tension in a tetanus as well as the difference in  $\text{Ca}^{2+}$  sensitivity of force and stiffness and more rapid phase 2 tension recovery ( $r$ ) at low  $\text{Ca}^{2+}$  activation. To characterize the contribution of myofilament compliance to sarcomere compliance and isometric force kinetics, the  $\text{Ca}^{2+}$ -activation dependence of sarcomere compliance in single glycerinated rabbit psoas fibers, in the presence of ATP (5.0 mM), was measured using rapid length steps. At steady sarcomere length, the dependence of sarcomere compliance on the level of  $\text{Ca}^{2+}$ -activated force was similar in form to that observed for fibers in rigor where force was varied by changing length. Additionally, the ratio of stiffness/force was elevated at lower force (low  $[\text{Ca}^{2+}]$ ) and  $r$  was faster, compared with maximum activation. A simple series mechanical model of myofilament and cross-bridge compliance in which only strong cross-bridge binding was activation dependent was used to describe the data. The model fit the data and predicted that the observed activation dependence of  $r$  can be explained if myofilament compliance contributes 60–70% of the total fiber compliance, with no requirement that actomyosin kinetics be  $[\text{Ca}^{2+}]$  dependent or that cooperative interactions contribute to strong cross-bridge binding.

## INTRODUCTION

Upon activation, skeletal muscle develops force that is accompanied by an increase in fiber and sarcomere stiffness ( $K_S$ ) and a corresponding decrease in compliance ( $C_S = 1/K_S$ ). The decrease in  $C_S$  upon activation has been attributed to increased interaction of myosin cross-bridges with actin (Ford et al., 1981). This interpretation was justified by the observations that 80–90% of fiber compliance could be attributed to cross-bridges, with the remaining fraction being attributed to other structural elements in series with the cross-bridges, such as z-bands, thick and thin filaments, and cytoskeletal elements (Ford et al., 1981; Bagni et al., 1988; Tawada and Kimura, 1984). Subsequently, measurements of  $K_S$  and  $C_S$  have been used to describe the strength of binding and distribution of actomyosin cross-bridges between mechanochemical states. For example, the dissociation of force and stiffness during the rise of force in a tetanus (Ford et al., 1986; Bagni et al., 1988), at steady submaximal force (Martyn and Chase, 1995) and force inhibition with phosphate (Pi) (Martyn and Gordon, 1992; Regnier et al., 1995; Dantzig et al., 1992), have been interpreted to indicate the presence of attached non-force-generating states in the cross-bridge cycle. However, evidence that a significant fraction (50–70%) of fiber compliance is attributable to the elastic properties of the thick and thin filaments (Higuchi et al., 1995; Huxley et al., 1994; Linari et al., 1998; Wakabayashi et al., 1994; Kojima et al., 1994)

raises new questions about interpretation of muscle mechanical data.

The presence of a substantial non-cross-bridge compliance would result in a partition of an applied length change between cross-bridges and the compliant structures in series with them (Higuchi et al., 1995). For example, when force is low because there are relatively few strongly bound cross-bridges (e.g., low  $\text{Ca}^{2+}$  activation or in the presence of inhibitors) the change in length of the most compliant structure, in this case cross-bridges, would be disproportionately larger than for less compliant structures. Likewise, as the degree of cross-bridge interaction and force increases, the relative compliance of that component decreases and a greater fraction of any length change is applied to the myofilament component of fiber compliance. As a consequence, when a rapid step decrease in sarcomere length (SL) is applied to the fiber, the amplitude necessary to cause force development by cross-bridges to drop to zero ( $Y_0$ ) (Huxley and Simmons, 1971, 1972) would be smaller at lower levels of force. A decrease in  $Y_0$  and the corresponding increase in the stiffness/force ratio could be explained by the presence of a large compliance in series with cross-bridges and not necessarily by redistribution between cross-bridge states (Martyn and Chase, 1995; Martyn and Gordon, 1992). Luo et al. (1994) have further suggested that myofilament compliance in series with an activation-dependent cross-bridge compliance could result in slower tension transients. Thus, at lower forces myofilament compliance would be less than cross-bridge compliance and tension transients would be faster than at higher forces, where more of the total fiber compliance would be attributable to cross-bridges. This could explain the inverse relation between force and the rate of phase 2 tension recovery ( $r$ ) when

Submitted April 16, 2002, and accepted for publication July 22, 2002.

Address reprint requests to Dr. Donald A. Martyn, Department of Bioengineering, Box 357962, University of Washington, Seattle, WA 98195. Tel.: 206-543-4478; Fax: 206-685-3300; E-mail: dmartyn@u.washington.edu.

© 2002 by the Biophysical Society

0006-3495/02/12/3425/10 \$2.00

steady force is altered either by  $\text{Ca}^{2+}$  (Martyn and Chase, 1995) or Pi (Martyn and Gordon, 1992), as well as during the rise of tetanic tension in intact fibers (Ford et al., 1986; Bagni et al., 1988; Linari et al., 1998).

To test whether a significant non-cross-bridge compliance can explain the activation dependence of  $C_S$ ,  $Y_0$ , and  $r$  we measured the dependence of fiber stiffness and  $r$  on the level of isometric force when force was varied by changing  $[\text{Ca}^{2+}]$ , was inhibited with  $\text{AlF}_4^-$  at maximal activating  $[\text{Ca}^{2+}]$  (Chase et al., 1994), or was activated in the absence of  $\text{Ca}^{2+}$  with a modified form of cardiac troponin C (aTnC) (Hannon et al., 1993). To minimize any change in compliance that might result from changes in myofilament overlap (Higuchi et al., 1995), particular care was taken to maintain steady SL constant throughout contractures. At steady SL,  $C_S$  and  $Y_0$  decreased at low forces and phase 2 tension transients ( $r$ ) were faster compared with maximum activation.

The data were fit with a simple model in which sarcomere stiffness is distributed between thick and thin filaments and all other sarcomeric structures ( $K_{\text{myo}}$ ), in series with the stiffness of the population of interacting cross-bridges ( $K_X$ ), which depends on the level of thin filament activation. This model is similar to that used by Luo et al. (1994) and Higuchi et al. (1995) to describe their results, with the addition of a viscous element (coefficient of viscosity =  $\eta_X$ ), which simplistically simulates a kinetic component. The model accurately described the force dependence of isometric phase 2 kinetics ( $r$ ) whether force was modulated by varying  $[\text{Ca}^{2+}]$ , by inhibition with alumino-fluoride ( $\text{AlF}_4^-$ ) in the presence of saturating  $[\text{Ca}^{2+}]$  or when fibers were activated in the absence of  $\text{Ca}^{2+}$  and predicted that the myofilament compliance was 60–76% of  $C_S$ .

## MATERIALS AND METHODS

Rabbits were housed in the Department of Comparative Medicine at the University of Washington and cared for in accordance with the U.S.A. National Institutes of Health Policy on Humane Care and Use of Laboratory Animals. All protocols were approved by the University of Washington Animal Care Committee.

### Fiber preparation

Segments of single muscle fibers from glycerinated rabbit psoas were prepared as described elsewhere (Chase and Kushmerick, 1988). Rabbits were first sedated with ketamine (40 mg  $\text{kg}^{-1}$ ) and xylazine (5 mg  $\text{kg}^{-1}$ ) and then anesthetized by continuous perfusion with ketamine (19.4 mg  $\text{ml}^{-1}$ ) and xylazine (0.83 mg  $\text{ml}^{-1}$ ) in saline through the marginal ear vein. Fiber end compliance was minimized by regional micro-application of 1% glutaraldehyde (Chase and Kushmerick, 1988). Isolated fiber segments were treated with 1% Triton X-100 in pCa 9.2 solution for 10 min to ensure perforation of membranous elements. Fiber segments were attached via aluminum foil T-clips to small wire hooks on the mechanical apparatus. After each experiment, we determined the total length of the two chemically fixed regions at the ends of the fiber segment, as described (Chase and

Kushmerick, 1988); the total fixed length was subtracted from the overall length to obtain the unfixed fiber length ( $L_F$ ). Variations in  $C_S$  and the kinetics of phase 2 tension recovery with pCa, and thus isometric force level, could not be attributed to activation-dependent alterations in myofilament lattice spacing that occur in skinned fiber preparations (Brenner, 1983), because these force-dependent changes in lattice spacing were minimized by the presence of 4% w/v Dextran T-500 in all solutions (see Solutions) (Matsubara et al., 1985). At  $\text{SL} = 2.45 \pm 0.01 \mu\text{m}$  (mean  $\pm$  SEM;  $n = 7$  fibers) fiber diameter was  $53.5 \pm 4.0 \mu\text{m}$  at pCa 9.2 and was unchanged at pCa 4.0.

### Mechanical apparatus

Force was measured with an AE 801 (Aksjeselkapet Mikro-elektronikk, Horten, Norway) force transducer (peak-to-peak noise equivalent to 0.3 mg; resonant frequency, 7 kHz). A Cambridge Technology (Watertown, MA) model 300 servo motor ( $-3\text{-dB}$  amplitude response at 2.4 kHz) was used to control fiber length ( $L_F$ ). SL was continuously monitored by helium-neon laser diffraction as previously described (Chase et al., 1993). Steady-state SL and fiber diameter was determined at  $\times 400$  magnification.

### Data acquisition and control

Data were acquired during continuous, steady-state submaximal and maximal (pCa 4.0)  $\text{Ca}^{2+}$  activation. Fiber mechanical properties and structure were maintained during prolonged activation by applying transient release/restretch changes in  $L_F$  (Brenner, 1983). Measurements of isometric force, sarcomere stiffness ( $K_S$ ), and force transient kinetics were made during the steady-state period between the Brenner cycles of unloading/restretch. The force baseline for each condition was determined during a large-amplitude, slack release. Fiber force was normalized to cross-sectional area, calculated from the diameter assuming circular geometry.

Both sarcomere stiffness ( $K_S$ ) and kinetics of the early phase of force recovery were determined from force and SL responses to rapid, step changes in  $L_F$  (Ford et al., 1977; Huxley and Simmons, 1972; Martyn and Chase, 1995). Step changes in  $L_F$  were implemented as 350-ms ramp changes in length. Signals were recorded by digitizing 2048 points with 12-bit resolution at a rate of 20 kHz per channel. To prevent aliasing, all signals were passed through a computer-controlled signal processor (CyberAmp 380; Axon Instruments, Foster City, CA) and filtered at 40% of the sampling frequency.  $K_S$  was determined from the slope of the relation between the maximum change in force ( $T_1$ ) following the  $L_F$  step and the corresponding change in SL ( $-4 < \Delta\text{SL} < 8 \text{ nm (h s)}^{-1}$ ) (Chase et al., 1993; Martyn and Chase, 1995). The  $\Delta\text{SL}$  intercept of this relationship ( $Y_0$ ,  $\text{nm (h s)}^{-1}$ ) was obtained by extrapolation of this regression to the ordinate.  $T_1$  was normalized to cross-sectional area ( $\text{mN mm}^{-2}$ ) and  $\Delta\text{SL}$  was normalized to the initial SL.  $K_S$  ( $\text{MPa} = 10^6 \text{ N m}^{-2}$ ), was determined and sarcomere compliance ( $C_S$ ) expressed as  $K_S^{-1} \times (\text{SL}_i/2) \times 1000$  ( $\text{nm (h s)}^{-1}) \times (\text{kN M}^{-2})^{-1}$ ), where  $\text{SL}_i$  is the initial SL ( $\mu\text{m}$ ).

The unprocessed, digitized data were analyzed using custom software. Reduced data were further analyzed by linear least-squares regression (Excel version 4.0 for Windows, Microsoft Corp., Redmond, WA) or by nonlinear least-squares regression (SigmaPlot version 4.1, Jandel Scientific, San Rafael, CA). Statistical analyses were performed using Excel (version 4.0 for Windows, Microsoft Corp., Redmond, WA). Student's  $t$ -test was used to compare data, with differences considered significant at the 95% confidence level ( $p < 0.05$ ).

### Solutions

Relaxing and activating solutions were prepared as described previously (Martyn and Chase, 1995) and contained 5 mM  $\text{Mg}^{2+}$ -ATP, 15

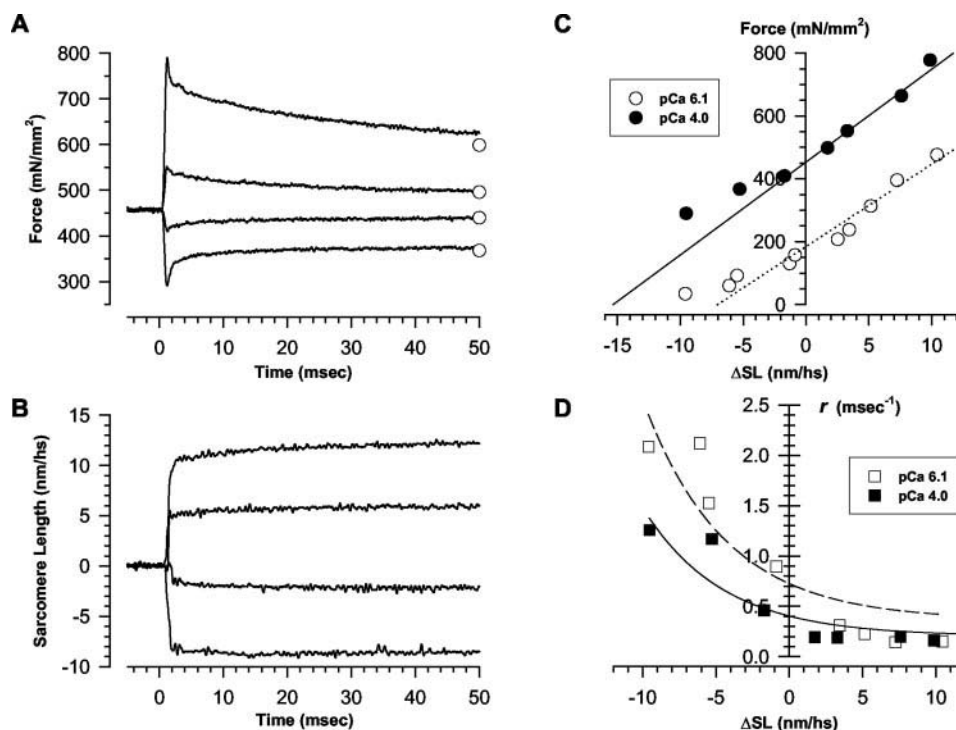


FIGURE 1 Transient changes in force (*A*) and SL (*B*) resulting from steps in fiber length applied to a single activated rabbit psoas fiber. SL remained relatively steady following each length step. The peak change in force ( $T_1$ ) was followed by a rapid partial recovery (phase 2) toward a steady force ( $T_2$ ), before the final recovery to the isometric level of force (not shown).  $T_2$  is indicated by the open circles to the right of the corresponding force traces in *A*. To determine  $C_s$  ( $1/K_s$ ) at each steady SL force level, changes in  $T_1$  were plotted against the corresponding changes in SL, and  $K_s$  was determined from the slope of the relationship, as illustrated in *C*.  $K_s$  was determined at maximal (pCa 4.0; ●) and submaximal activating  $[Ca^{2+}]$  (pCa 6.1; ○). For each condition  $Y_0$ , the amplitude of SL decrease necessary to decrease  $T_1$  to zero was determined by linear extrapolation of the  $T_1$ - $\Delta SL$  relationship between  $\pm 4.0$  nm (h s)<sup>-1</sup> (*C*). In *D*, the dependence of phase 2 tension recovery rate ( $r$ ) on the amplitude of the step in SL at pCa 4.0 (■) and 6.1 (□) is illustrated.

mM phosphocreatine (PCr), 15 mM EGTA, at least 40 mM MOPS, 135 mM Na<sup>+</sup> + K<sup>+</sup>, 1 mM Mg<sup>2+</sup>, pH 7.0, 250 U/ml creatine phosphokinase (CK), and Dextran T-500 (4% w/v; Pharmacia, Piscataway, NJ). To alter solution  $[Ca^{2+}]$ , varying amounts of calcium propionate were added as determined with a computer program taking into account the desired free  $[Ca^{2+}]$  and the binding constants of all solution constituents for  $Ca^{2+}$ ; ionic strength was maintained constant (200 mM) by varying [MOPS] appropriately at each pCa. The experimental temperature was 10–11°C and varied by <1°C during an experiment.

## RESULTS

### $[Ca^{2+}]$ dependence of fiber compliance and $Y_0$

When force and SL reached steady levels during  $Ca^{2+}$  activation, stiffness was measured by applying rapid length steps to the fibers (Huxley and Simmons, 1972; Ford et al., 1977), as illustrated in Fig. 1. Maximum  $Ca^{2+}$ -activated (pCa 4.0) control force was  $390 \pm 33.0$  mN mm<sup>-2</sup> at SL =  $2.45 \pm 0.01$   $\mu$ m (mean  $\pm$  SD;  $n = 7$  fibers). For the same fibers, relaxed force (pCa. 9.2) was  $1.7 \pm 0.5\%$  of the maximum.

Transient changes in force (Fig. 1 *A*) and SL (Fig. 1 *B*) resulting from steps in  $L_F$  from a single  $Ca^{2+}$ -activated rabbit psoas fiber are shown. During transient measure-

ments, SL remained steady at each  $L_F$ . Following each step, the peak change in force ( $T_1$ ) was followed by a rapid partial recovery (phase 2) toward a steady force ( $T_2$ ), before the final recovery to the isometric level of force (not shown).  $T_2$  is indicated by the open circles to the right of the corresponding force traces in the top panels of Fig. 1 *A*. To determine  $C_s$  ( $1/K_s$ ) at each steady SL and force level, changes in  $T_1$  were plotted against the corresponding changes in SL, and the slope of the relationship ( $K_s$ ) was determined, as illustrated in Fig. 1 *C*. For each condition  $Y_0$ , the amplitude of SL decrease that was large enough to cause  $T_1$  to drop to zero was determined by linear extrapolation of the  $T_1 - \Delta SL$  relationship between  $-4.0$  and  $+6.0$  nm (h s)<sup>-1</sup>. In Fig. 1 *D* the dependence of phase 2 tension recovery rate ( $r$ ) on the amplitude of the step in SL is illustrated for the experiment shown in Fig. 1 *C*. Because phase 2 tension recovery is not accurately described by a single exponential (Davis and Rodgers, 1995), the rate of tension recovery from  $T_1$  to  $T_2$  was characterized by the time required for tension to change from  $T_1$  by 50% of the difference between  $T_1$  and  $T_2$  ( $r = t_{0.5}^{-1}$ ).

At each  $[Ca^{2+}]$  the  $\Delta SL$  dependence of  $r$  (for stretches and releases) was modeled as described by Huxley and Simmons (1971). In this model, during force generation cross-bridges are in equilibrium between two attached states. The distribution between these states is determined by a forward rate constant ( $k^+$ ) that is dependent on cross-bridge strain and a reverse rate constant ( $k^-$ ) that is strain independent. The relation between  $k^+$  and  $k^-$  was defined as  $k^+ = k^- (e^{-yKh/kT})$ , where  $y$  is the cross-bridge extension,  $K$  is the cross-bridge stiffness,  $h$  is the cross-bridge motion associated with the transition,  $k$  is the Boltzman constant, and  $T$  is the temperature. The rate of transition to a new equilibrium distribution is  $r = k^+ + k^-$ , or:

$$t_{0.5}^{-1} \approx r = k^- (1 + e^{-yKh/kT}) = k^- (1 + e^{-y\alpha}), \quad (1)$$

where  $\alpha = Kh/kT$ . Data from each fiber were fit using nonlinear regression analysis to Eq. 1 (Huxley and Simmons, 1971) (Fig. 1 D), yielding the value of  $k^-$  and  $\alpha$ . As found for both intact frog skeletal fibers (Ford et al., 1977) and skinned rabbit psoas fibers (Martyn and Chase, 1995), Eq. 1 did not completely describe the  $r$ - $\Delta SL$  relation, tending to over estimate  $r$  for larger stretches.

The relationship between  $C_s$  and force at varying  $[Ca^{2+}]$  obtained at an SL of  $2.47 \pm 0.01 \mu m$  (mean  $\pm$  SEM;  $n = 7$  fibers) is summarized in Fig. 2 A. The results are similar in appearance to those obtained by Higuchi et al. (1995) where cross-bridge strain was altered in fibers in the rigor state. At maximal force levels our values of  $C_s$  are  $\sim 55\%$  of that observed for skinned rabbit psoas fibers in rigor (Higuchi et al., 1995). The  $[Ca^{2+}]$  dependence of  $Y_0$  corresponding to the values of  $C_s$  in Fig. 2 A is described in Fig. 2 B.  $Y_0$  increased as the level of force increased, as we have previously shown (Martyn and Gordon, 1992; Martyn and Chase, 1995). At maximal levels of  $Ca^{2+}$ -activated force the value of  $Y_0$  was  $-9.8 \pm 0.5 \mu m$  (mean  $\pm$  SEM;  $n = 7$  fibers). Interestingly, at low levels of isometric force the value of  $Y_0$  extrapolated to  $\sim 4$  nm per half-sarcomere, a value that is similar to that measured for the power stroke of single isolated myosin motors (Malloy et al., 1995). The results in Fig. 2 B can be described by the regression  $Y_0 = Y_{\min} + Y_{\max} (f(K_X^*/K_{myo}))$ , where  $Y_{\min}$  and  $Y_{\max}$  are the values of  $Y_0$  extrapolated to minimal and maximum levels of activation and  $f$  is the normalized value of isometric force. Thus, the activation dependence of  $Y_0$  could be explained if at pCa 4.0 ( $f = 1.0$ ) the ratio of  $K_X^*/K_{myo}$  was 0.40 (4.0 nm/10.0 nm), so that of the applied 10 nm ( $h$  s) $^{-1}$  step, only 40% was taken up by cross-bridges with the remainder being applied to the myofilaments. This analysis assumes that  $K_{myo}$  is not activation dependent. The results in Fig. 2 B are similar to recent data from frog intact skeletal muscle fibers in which the isometric force dependence of stiffness and  $Y_0$  was measured (Linari et al., 2002). However, the value of  $Y_0$  at pCa 4.0 obtained

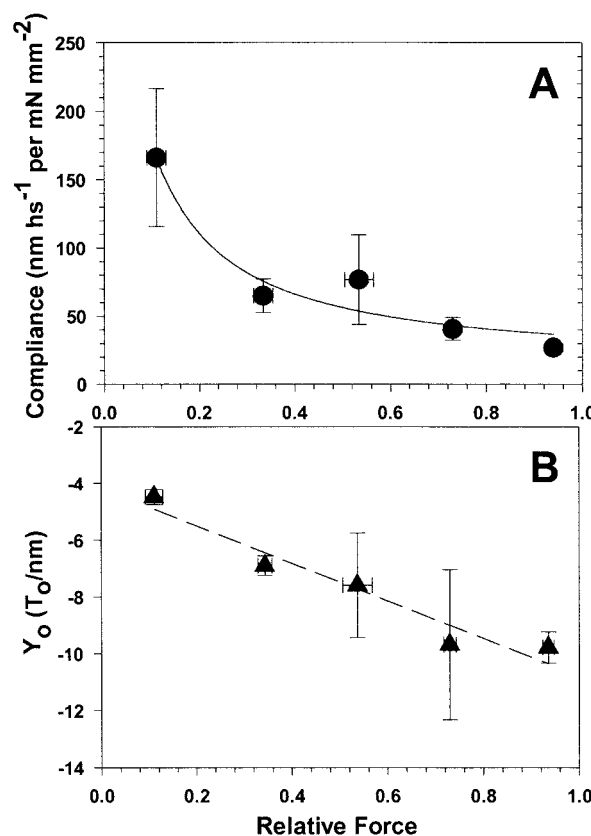


FIGURE 2 (A) The relationship between sarcomere compliance ( $C_s$ ) and relative force obtained at  $2.47 \pm 0.01 \mu m$  SL ( $\bullet$ ; mean  $\pm$  SEM;  $n = 7$  fibers). Data were binned in intervals of 20% relative force. Submaximal forces are normalized to force at pCa 4.0. (B) Dependence of  $Y_0$  ( $\blacktriangle$ ) on  $Ca^{2+}$ -activated force for the data in A. The results in B were fit by line regression to the equation  $Y_0 = Y_{\min} + Y_{\max} \times (f(K_X^*/K_{myo}))$  (---), where  $Y_{\min}$  and  $Y_{\max}$  are the values of  $Y_0$  extrapolated to minimal and maximum levels of activation. Regression parameter estimates are given in Results.

from psoas skinned fibers at  $10^\circ C$  (Table 1) is larger than reported for frog intact fibers at lower temperatures ( $4-5$  nm ( $h$  s) $^{-1}$ ) (Piazzesi et al., 1992). This difference is probably less because decreasing temperature causes a decrease in maximal  $Ca^{2+}$ -activated force in rabbit skinned psoas fibers (Ranatunga, 1996). Thus, skinned psoas fibers at  $0-5^\circ C$  would generate  $\sim 50\%$  less force and, referring to Fig. 2 B at 50% relative force,  $Y_0$  would decrease to  $\sim 7.5$  nm ( $h$  s) $^{-1}$ .

### $[Ca^{2+}]$ dependence of phase 2 kinetics

The dependence of  $r$  on  $\Delta SL$  was determined at different activating  $[Ca^{2+}]$  (pCa 6.4–4.0) and fit with Eq. 1, yielding values of  $k^-$  and  $\alpha$ . In Fig. 3 the  $r$ - $\Delta SL$  relation is compared for data pooled from six fibers when force was  $34.0 \pm 2.0\%$  ( $\blacktriangle$ ) and  $94.0 \pm 2.0\%$  ( $\bullet$ ) of maximum (pCa 4.0). The value of  $r$  at its y-axis intercept is twice the value of  $k^-$  (Huxley and Simmons, 1971, 1972). The data in Fig. 3 indicate that



**TABLE 1** The dependence of the rate of tension recovery during phase 2 of the transient force response to a quick step in SL on the size of the length step was fit with Eq. 2

| Condition                      | <i>n</i> | Relative force | $k^-$       | $Kh/kt$     | $Y_0$        |
|--------------------------------|----------|----------------|-------------|-------------|--------------|
| Ca                             | 7        | 0.14 ± 0.01    | 0.57 ± 0.05 | 0.16 ± 0.01 | -4.47 ± 0.27 |
| Ca                             | 6        | 0.34 ± 0.01    | 0.37 ± 0.06 | 0.19 ± 0.01 | -6.90 ± 0.34 |
| Ca                             | 6        | 0.50 ± 0.03    | 0.32 ± 0.05 | 0.22 ± 0.02 | -7.58 ± 1.80 |
| Ca                             | 5        | 0.73 ± 0.01    | 0.27 ± 0.04 | 0.25 ± 0.06 | -9.70 ± 2.60 |
| Ca                             | 7        | 0.93 ± 0.02    | 0.27 ± 0.04 | 0.19 ± 0.02 | -9.80 ± 0.55 |
| Ca (AlF <sup>4-</sup> control) | 5        | 0.99 ± 0.01    | 0.42 ± 0.08 | 0.20 ± 0.03 | -12.9 ± 2.80 |
| Ca (post-recovery)             | 4        | 0.78 ± 0.02    | 0.39 ± 0.06 | 0.28 ± 0.03 | -10.5 ± 0.59 |
| Ca (during recovery)           | 3        | 0.22 ± 0.07    | 0.75 ± 0.11 | 0.18 ± 0.02 | -6.8 ± 0.56  |
| 200 μm AlF <sup>4-</sup>       | 2        | 0.16 ± 0.20    | 0.65 ± 0.10 | 0.14 ± 0.04 | -3.8         |
| 500 μm AlF <sup>4-</sup>       | 5        | 0.03 ± 0.01    | 0.91 ± 0.09 | 0.16 ± 0.03 | -3.2 ± 0.24  |
| aTnC (4.0 control)             | 2        | 1              | 0.30 ± 0.08 | 0.27 ± 0.05 |              |
| Part aTnC (9.2)                | 2        | 0.26 ± 0.01    | 0.55 ± 0.01 | 0.30 ± 0.03 |              |
| Full aTnC (9.2)                | 2        | 0.67 ± 0.01    | 0.25 ± 0.04 | 0.34 ± 0.03 |              |

Data were obtained from experiments in which steady isometric force was altered by changing [Ca<sup>2+</sup>], by inhibiting force with aluminofluoride (AlF<sup>4-</sup>), or by selective reconstitution of skinned fibers with a constitutively activating cardiac TnC (aTnC) in the absence of Ca<sup>2+</sup>.

tension recovery during tension transient phase 2 is faster at lower levels of force, as previously described (Martyn and Chase, 1995; Bagni et al., 1988, 1999).

# The model

To test whether the Ca<sup>2+</sup>-activation dependence of *r*, described in Figs. 1–3, results primarily from the presence of a significant myofilament compliance and not from an activation depen-

dence of cross-bridge kinetics, we propose a model that predicts the fraction of total *C<sub>s</sub>* due to myofilaments necessary to describe the data. The model consists of two elastic components *K<sub>myo</sub>* and *K<sub>x</sub>* in series with a kinetic element, represented by a dash pot with viscosity *η<sub>x</sub>* (Fig. 4 *A*). *K<sub>myo</sub>* represents all components of elasticity with the sarcomere other than that of the population of cross-bridges in the overlap zone between thick and thin filaments, whereas *K<sub>x</sub>* represents the cross-bridge component of elasticity that can vary with the level of strong actomyosin interaction (Fig. 4 *A*). We have made no attempt to model the distribution of myofilament strain along the overlap zone (Daniel et al., 1998; Mijailovich et al., 1996)

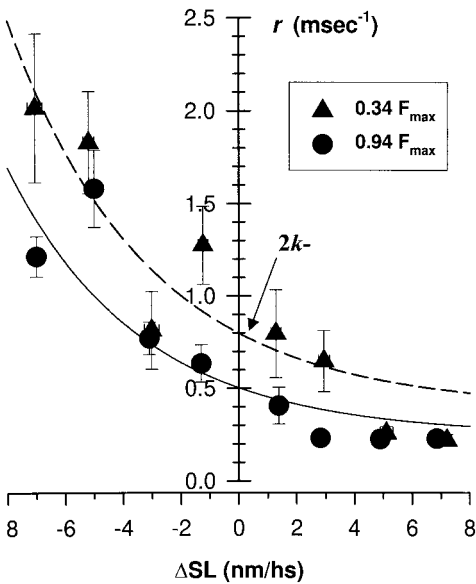


**FIGURE 3** Dependence of the rate of tension recovery following step changes in fiber length (*r*) upon the corresponding SL changes. Data were pooled from six fibers at 94% ± 2.0% (●) and 34% ± 2.05 (▲) maximum Ca<sup>2+</sup>-activated force (mean ± SEM; *n* = 6 fibers). At each force level, the *r*-ΔSL relation was fit by Eq. 1 (dashed and solid lines). The intercept of the data for each force level on the *y* axis is equal to 2 *k*<sup>-</sup>, as indicated in the figure (arrow).

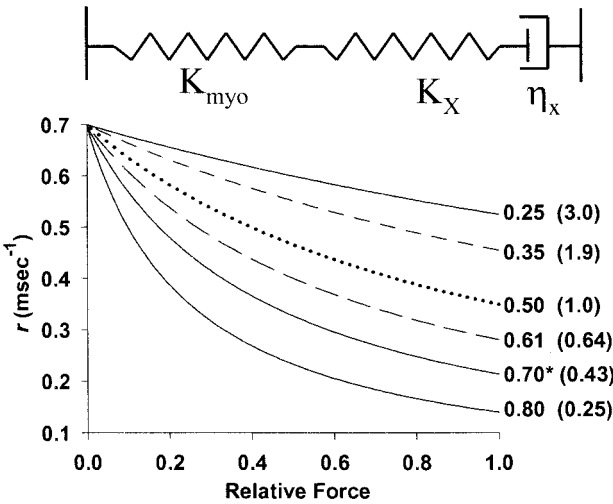


**FIGURE 4** (*A*) Schematic illustration of the series components of the model (see Results). (*B*) The force or activation dependence of *r* was generated using Eq. 2 for a range of *β* values; the values of myofilament compliance as a fraction of *C<sub>s</sub>* at maximum Ca<sup>2+</sup> activation are given to the right of each curve (*1/K<sub>myo</sub>*/(*1/K<sub>myo</sub>* + *1/K<sub>x</sub>*)), with the corresponding value of *β* (*K<sub>myo</sub>*/*K<sub>x</sub>*) in parentheses.

because to do so would require knowledge of the fraction of strong cross-bridges at maximum activation.

Increasing  $[Ca^{2+}]$  enhances strong actomyosin interaction, increasing both the relative stiffness of the cross-bridge component ( $K_X$ ; Figs. 1 and 2) and the apparent viscosity ( $\eta_X$ ; Fig. 3). Length changes applied to the ends of the fiber or sarcomere will be partitioned preferentially to the more compliant of the two components. Thus, if  $K_{myo}$  is not significantly dependent on the level of activation, increasing force and  $K_X$  (decreasing cross-bridge compliance) would result in a smaller fraction of the applied length change being applied to the cross-bridge population, causing an apparent increase in the amplitude of length step required to drop force to zero ( $Y_0$ ) as the level of activation and force rises (Fig. 2). In addition, the model predicts that with the damped element  $\eta_X$ , a step change in overall length results in a transient change of force following the step that has a time constant  $\tau = K/\eta_X$  and a rate  $r = 1/\tau$ . Because stiffness and compliance are distributed between two components,  $r$  is dependent on the ratio  $K_{myo}/K_X$ , as follows.

1) If  $K_X \ll K_{myo}$ , then

$$r' = 1/\tau = K_X/\eta_X$$

2) Assuming that  $K_X$  and  $\eta_X$  vary in proportion to normalized force ( $f$ ), so that  $K_X = f_X^*$  and  $\eta_X = f\eta_X^*$  ( $K_X^*$  and  $\eta_X^*$  are the values at maximum  $Ca^{2+}$  activation), then

$$r' = fK_X^*/f\eta_X^*$$

and thus  $r'$  would be independent of activation level.

3) On the other hand, if  $K_{myo}$  is closer in value to  $K_X$ , for the series combination of  $K_{myo}$  and  $K_X$ :

$$r = (K_{myo} \cdot K_X)/((K_{myo} + K_X)(\eta_X))$$

4) Let  $\beta$  be the proportionality between  $K_{myo}$  and  $K_X^*$  ( $\beta = K_{myo}/K_X^*$ ), then substitution into the third equation above yields:

$$r' = Z\beta/(\beta + f), \quad (2)$$

where  $Z = (K_X^*/\eta_X^*)$ .

The model predicts that  $r$  should change inversely with the level of isometric force, as found experimentally (Figs. 1–3). To illustrate the behavior of the model, curves describing the activation dependence of  $k^-$  were generated using a range of  $\beta$  values are shown in Fig. 4 B. For larger  $\beta$ ,  $r$  has little dependence on force, whereas for smaller values of  $\beta$ ,  $r$  becomes more strongly force dependent. The ratio  $Z$  ( $K_X^*/\eta_X^*$ ) is the y-axis intercept at zero force. This simple analysis indicates that any maneuver that causes either a decrease in force or an apparent increase in  $K_{myo}$  could decrease  $Y_0$  (increased the stiffness/force ratio; see Fig. 2 B) and increase  $r$ , without any need to hypothesize an activation dependence of cross-bridge kinetics or cooperative interactions (Martyn and Chase, 1995; Bagni et al., 1988). Furthermore, by determining the force dependence of  $r$  and fitting the model to the data we can

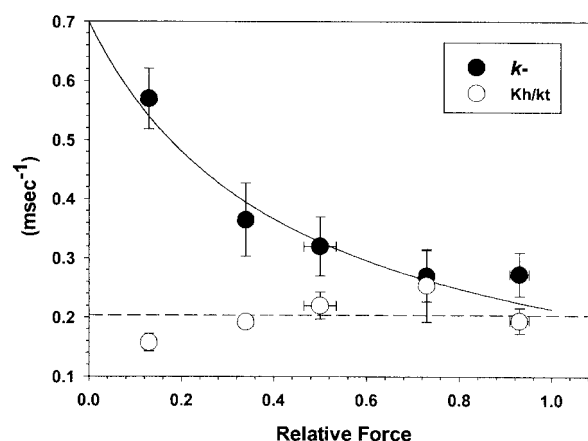


FIGURE 5 The  $Ca^{2+}$ -activation dependence of the  $r$ - $\Delta SL$  (as in Fig. 3) relation was determined over a range of  $[Ca^{2+}]$  for seven fibers. For each fiber the values of  $k^-$  (●) and  $Kh/kt$  (○) at each  $[Ca^{2+}]$  were obtained by nonlinear regression analysis of the data with Eq. 1. The pooled data are included in Table 1. The values of  $k^-$  in Fig. 5 were fit by Eq. 2 (solid curve), and the calculated values of  $\beta$  (0.44) and  $Z$  are included in Table 2.

calculate  $\beta$  and thereby the possible partition of  $C_S$  between the myofilament and cross-bridge components in skinned fibers.

### Fitting the model to the activation dependence of $r$

Fig. 5 illustrates that  $k^-$  increased with decreasing activation and  $\alpha$  was relatively independent of activation level, as previously observed (Martyn and Chase, 1995). As suggested in the Introduction an increase in  $r$  (or  $k^-$ ) could result from the presence of a substantial myofilament compliance. To determine the degree of filament compliance necessary to fit the data in Fig. 5, pooled values of  $k^-$  were obtained at different levels of  $Ca^{2+}$  activation and fit by Eq. 2. The value of  $\beta$  necessary to fit the data was  $0.44 \pm 0.12$  (mean  $\pm$  SEM;  $n = 7$  fibers) for  $Ca^{2+}$ -activated contractions corresponding to a fractional myofilament compliance of  $0.69 C_S$ , a value that is similar to direct measurements of actin filament compliance (Kojima et al., 1994), fiber compliance in rigor (Higuchi et al., 1995), and x-ray diffraction measurements of meridional myofilament reflections (Wakabayashi et al., 1994; Huxley et al., 1994). The values of  $k^-$  obtained at different levels of  $Ca^{2+}$  activation are included in Table 1.

### Force dependence of $k^-$ when tension is altered by alumino-fluoride or in the absence of $Ca^{2+}$

The ability of the model to fit the data and yield values of myofilament compliance (Fig. 5; Table 1) that are comparable to that obtained by more direct measurements of myofilament compliance suggests that the activation depen-

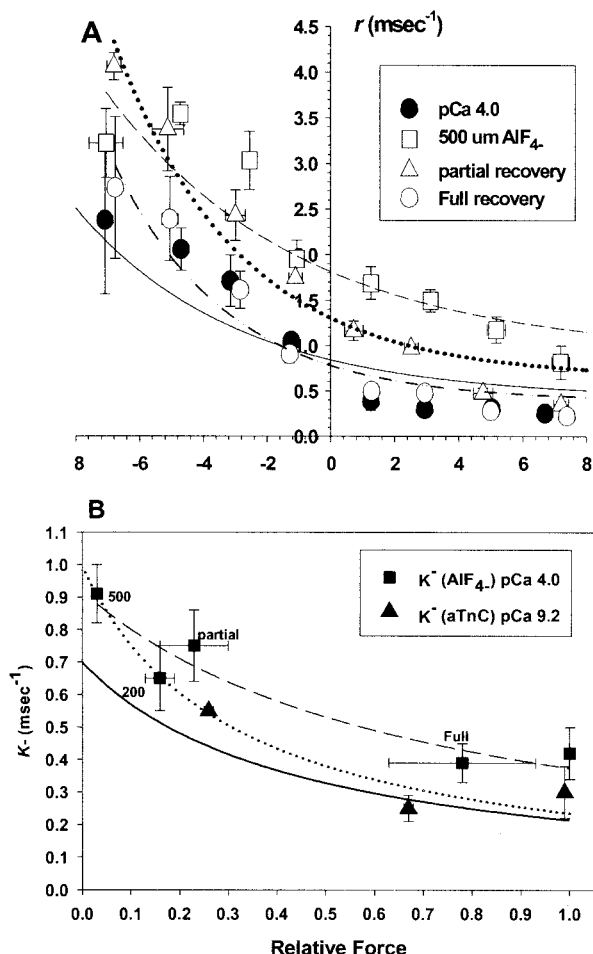


FIGURE 6 (A) As described for Figs. 1 and 3, the  $r$ - $\Delta SL$  relation was measured in controls (●, —) and when force was inhibited with 0.5 mM AIF<sub>4</sub><sup>-</sup> (□, — — —) in pCa 4.0 activating solution (means  $\pm$  SEM;  $n = 7$  fibers) and allowed to recover from inhibition (○, ···). Also, from three fibers of this set data were obtained during partial recovery from force inhibition (△; dashed, double dotted line). The values of  $k^-$  and  $\alpha$  for each condition were determined by fitting the data in A with Eq. 1. (B) The force dependence of  $k^-$  derived from the data in A is shown (■) along with the curves fits from Eq. 2 (— — —). As described in Results, data from two fibers reconstituted with low and high levels of aTnC in the absence of Ca<sup>2+</sup> (▲; ···) are also included and fit by Eq. 2. The calculated values of  $\beta$  for the data in B are included in Table 2. For comparison, the fit curve to the  $k^-$  data in Fig. 5 is included (—).

dence of  $r$  may result directly from altered cross-bridge binding and force, rather than from effects of Ca<sup>2+</sup> per se on cross-bridge kinetics. To test this idea in a subset of fibers we inhibited force at pCa 4.0 with alumino-fluoride (AIF<sub>4</sub><sup>-</sup>; 0.5 mM Al(NO<sub>3</sub>)<sub>3</sub> plus 10 mM F), a phosphate analog that binds to myosin with slow dissociation kinetics (Chase et al., 1994; Smith and Rayment, 1995). As described for Figs. 1 and 3, in Fig. 6 A the  $r$ - $\Delta SL$  relation was measured in three fibers when force was inhibited with AIF<sub>4</sub><sup>-</sup> (0.5 mM; □) in pCa 4.0 activating solution and at submaximal force during partial recovery from inhibition when the fibers were activated in pCa 4.0 solution with no AIF<sub>4</sub><sup>-</sup> (△). Finally,

TABLE 2 The relationship of  $k^-$  to relative force was fit with Eq. 1 for the conditions described in Table 1

| Condition                     | $n$ | $\beta$         | $Z$             | % Compliance |
|-------------------------------|-----|-----------------|-----------------|--------------|
| Ca                            | 7   | $0.44 \pm 0.12$ | $0.72 \pm 0.08$ | 69           |
| AIF <sub>4</sub> <sup>-</sup> | *   | $0.68 \pm 0.21$ | $0.92 \pm 0.08$ | 60           |
| aTnC                          | 2   | $0.31 \pm 0.34$ | $1.0 \pm 0.60$  | 76           |

The corresponding derived values of  $\beta$ ,  $Z$ , and the fraction of total fiber compliance from sources other than crossbridges ( $\pm$ SEM) are listed.

\*See Legend for Figure 6.

force was allowed to maximally recover in pCa 4.0 with no AIF<sub>4</sub><sup>-</sup> (○). The values of  $k^-$  and  $\alpha$  for each condition were determined by fitting the data in Fig. 6 A with Eq. 1. The dependence of  $k^-$  on relative force is shown in Fig. 6 B along with the curves fits from Eq. 2. As shown in Fig. 3 at submaximal forces  $r$  and  $k^-$  are faster, whether force is modulated by changing [Ca<sup>2+</sup>] (Fig. 5) or by inhibition of force with AIF<sub>4</sub><sup>-</sup> in the presence of maximal [Ca<sup>2+</sup>] (Fig. 6 A). The calculated values of  $\beta$  for the conditions illustrated in Fig. 6 B are included in Table 2.

To further test the hypothesis that the apparent activation dependence of  $r$  and  $k^-$  does not result from altered thin filament Ca<sup>2+</sup> activation per se, data similar to that in Fig. 6 A were obtained when skinned skeletal fibers were activated with a modified cardiac TnC (aTnC) and are included in Fig. 6 B. Fibers were reconstituted with a modified form of cTnC (aTnC) in which endogenous cysteine residues 84 and 35 were cross-linked under oxidizing conditions (Hannon et al., 1993; Putkey et al., 1993). aTnC constitutively activated force in the absence of Ca<sup>2+</sup> (Hannon et al., 1993). The data shown were obtained from two fibers in which force and stiffness were measured when the fibers were fully and partially reconstituted with aTnC at pCa 9.2 (Hannon et al., 1993). As for modulation of force by changing [Ca<sup>2+</sup>] (Fig. 5) and inhibition with AIF<sub>4</sub><sup>-</sup> (Fig. 6, A and B),  $r$  and  $k^-$  increased when force was submaximal. The values of  $k^-$ ,  $\alpha$ , and  $\beta$  obtained with aTnC are included in Tables 1 and 2.

## DISCUSSION

The apparent decrease in phase 2 tension redevelopment kinetics ( $r$ ; Figs. 1, 3, and 5) and increase of  $Y_0$  (Fig. 2 B) as the level of Ca<sup>2+</sup>-activated force increases in skinned psoas fibers from rabbit is similar to that previously reported (Martyn and Chase, 1995). We originally interpreted those results as being consistent with either a Ca<sup>2+</sup> dependence of kinetic steps in the cross-bridge cycle related to phase 2 or a cooperative mechanism by which the probability of transition from attached but low-force states into strongly bound force-producing states increased as force increased (Bagni et al., 1988). Both these interpretations assume that the contribution of structures other than crossbridges to sarcomere compliance was no more than 10–20%

of  $C_S$  (Ford et al., 1986). However, direct measurements of isolated thin filament compliance (Kojima et al., 1994; Isambert et al., 1995), low-angle x-ray diffraction of fibers (Huxley et al., 1994; Wakabayashi et al., 1994), and the length dependence of  $C_S$  in the rigor state (Higuchi et al., 1995) all suggest that  $\sim 50\%$  of the  $C_S$  resides in the thin and thick filaments and other non-cross-bridge structures. Thus, it was necessary to determine whether the presence of a significant non-cross-bridge compliance could influence measurements of  $Y_0$  and phase 2 tension transients and the interpretations of the data. Our approach has been to develop a simple model (Results; Fig. 4) in which  $C_S$  is partitioned between two elastic elements,  $K_{\text{myo}}$ , which consists of contributions from thick and thin filaments, as well as other sarcomeric structures (z-bands, titin, etc.), and  $K_X$ , the elasticity of strongly bound actomyosin cross-bridges in the overlap zone between thin and thick filaments. By assuming that the level of  $\text{Ca}^{2+}$  activation had no direct effect on  $r$  and the apparent activation dependence of  $r$  (Figs. 1 A, 3, and 5) occurred only because  $K_{\text{myo}} \approx K_X$  during maximum activation, fitting Eq. 2 to the data (Figs. 4 and 5) yielded values of  $\beta$  ( $K_{\text{myo}}/K_X^*$ ) and myofilament compliance ( $0.60\text{--}0.76 C_S$ ; Table 2) that were consistent with measurements of myofilament stiffness made by mechanical measurements on isolated thin filaments and fibers in rigor and structural measurements on whole muscle. Furthermore, similar values of  $\beta$  were obtained by measuring the activation dependence of  $Y_0$  (Fig. 2 B; Table 1). These similarities suggest that the apparent activation or force dependence of  $Y_0$  and  $r$  could result primarily from the presence of a significant myofilament compliance and not from  $\text{Ca}^{2+}$  or activation dependence of cross-bridge transitions between cross-bridge states.

### Comparison of sarcomere compliance measurements in intact and skinned fibers

There is some conflict regarding the magnitude of non-cross-bridge compliance when measured mechanically in skeletal fibers. For example, compliance measurements made in intact frog fibers (Bagni et al., 1990; Ford et al., 1986; Linari et al., 1998) and glycerinated rabbit psoas fibers in rigor (Tawada and Kimura, 1984) indicate that only  $\sim 10\text{--}20\%$   $C_S$  results from non-cross-bridge structures, whereas the results of Higuchi et al. (1995) suggest a value of  $50\%$   $C_S$ . This conflict could result from differences between the various experimental approaches. In the experiments of Higuchi et al. (1995), SL was varied over a range where overlap between thin and thick filaments was constant for fibers in rigor; the compliance of that region was assumed to be invariant. In the study by Tawada and Kimura (1984) the degree of myofilament overlap and the compliance of the overlap region varied. A feature common to both procedures is that the length of the non-overlap region increased with increased SL. Analysis of the data

from Higuchi et al. (1995) lead to the conclusion that a very significant component of total compliance resided in the thin filaments, whereas the results of Tawada and Kimura (1984) are not consistent with a large non-cross-bridge component of compliance. In fact, the amount of non-cross-bridge compliance of skinned rabbit fibers in rigor, as determined at SL above  $2.5 \mu\text{m}$  (Tawada and Kimura, 1984), was the same as that described for intact electrically stimulated frog fibers (Bagni et al., 1990; Ford et al., 1986).

For fibers in rigor it was assumed that the compliance of the overlap region was constant and low, and only the compliance of the non-overlap region changed when SL is altered (Higuchi et al., 1995). In contrast, during active contractions the compliance of the overlap region would depend on the level of activation (Higuchi et al., 1995) and the number of interacting actomyosin cross-bridges (Gordon et al., 1966, 2000). It is noteworthy that the dependence of compliance on the level of isometric force in our activated fibers is similar in form to that observed in rigor (Higuchi et al., 1995). In both studies, compliance is highest at low force and decreases to a plateau at high forces. In our case, a portion of the high  $C_S$  at low forces is presumably due to the lower level of thin filament activation and actomyosin interaction (Fig. 2 A), whereas for fibers in rigor, the higher compliance at low degrees of cross-bridge strain must be attributed to the nonlinear properties of the non-overlap thin filament stress/strain relationship.

### Possible contribution of an activation-dependent $K_{\text{myo}}$

The model (Fig. 4) assumes that only the value of  $K_X$  depends on the level of thin filament activation. However, the flexural rigidity and stiffness of isolated thin filaments not only depends on the presence of regulatory complexes but is also altered by  $\text{Ca}^{2+}$  binding to TnC (Isambert et al., 1995; Kojima et al., 1994). The flexural rigidity of thin filaments, and presumably their axial stiffness, was found to be maximal in actin filaments reconstituted with tropomyosin and troponin, whereas the rigidity of these regulated filaments decreased by a factor of 2 when  $\text{Ca}^{2+}$  was bound to TnC, to that found for unregulated actin filaments (Isambert et al., 1995). Furthermore, the compliance of thin filaments determined by flexural rigidity was similar to that obtained by direct mechanical measurements of isolated actin filament compliance (Kojima et al., 1994). Thus, one could speculate that at lower levels of activation, thin filament compliance would decrease. At a given SL, this would result in a greater proportion of an applied length change being partitioned to the attached cross-bridges; i.e.,  $Y_0$  would decrease and the stiffness/force ratio increase at low activation, as observed (Fig. 2 B; Table 1).

If structural changes of the thin filament alter compliance, then cross-bridge binding could contribute to these changes as well. For example, thin filament activation is dependent



on and enhanced by strong cross-bridge binding in solution studies (McKillop and Geeves, 1993; Geeves and Lehrer, 1994). Thus, cycling cross-bridges could alter thin filament compliance in the overlap zone in a way analogous to  $\text{Ca}^{2+}$  binding (Isambert et al., 1995). Furthermore, this effect could extend into the non-overlap zone a fixed distance from the A-I band boundary; at shorter lengths this fixed distance would be a greater proportion of the I band. The recent observation that cross-bridge binding in the overlap zone between thick and thin filaments enhances binding of myosin S1 subfragments for a distance into the non-overlap I band (Swartz et al., 1996) supports this idea. Because cross-bridge binding is maximal in rigor, this effect could increase the apparent myofilament compliance of fibers in rigor (Higuchi et al., 1995). On the other hand, the relative fraction of strong, cycling cross-bridge binding during activation is a matter of controversy with estimates ranging from 10–15% (Allen et al., 1996; Howard, 1997; Daniel et al., 1998; Corrie et al., 1999) to 80% (Ford et al., 1986; Bagni et al., 1990). If the lower estimates of cycling cross-bridge binding are correct, it is unlikely that this small fraction could influence filament compliance by directly altering thin filament structure, whereas the opposite may be true if the higher estimates are found to be accurate.

Although  $\text{Ca}^{2+}$  binding and cross-bridge-induced changes in thin filament structure could increase thin filament compliance ( $\beta (K_{\text{myo}}/K_X^*)$  would vary with the level of contractile activation), our data indicate that this may not be the case. For example, the force dependence of  $Y_0$  (Table 1) and  $r$  (Figs. 1, 3, and 5) are similar whether force is changed by varying  $[\text{Ca}^{2+}]$  or by inhibition with  $\text{AlF}_4^-$  (Fig. 6, A and B; Table 2) in the presence of maximal  $[\text{Ca}^{2+}]$  (pCa 4.0). Although the data do not exclude an activation dependence of thin filament compliance, the finding that  $Y_0$  and  $r$  are similar at low force levels (Table 1), whether achieved with low  $[\text{Ca}^{2+}]$  or high  $[\text{Ca}^{2+}]$  with  $\text{AlF}_4^-$ , suggests that the contribution of activation- or  $[\text{Ca}^{2+}]$ -dependent changes in thin filament compliance to  $C_S$  is small.

### Consequences to measurements and interpretation of cross-bridge kinetics

If, as we propose, myofilament compliance has a significant influence of the apparent rate of phase 2 tension recovery ( $r$ ) then this should be extended to all measurements of cross-bridge kinetics, including  $k_{\text{TR}}$  (see Luo et al., 1994) and sinusoidal measurements of fiber stiffness (Kawai et al., 1981) obtained under conditions in which the degree of cross-bridge binding is altered. For example, inspection of Eq. 2 indicates that at any force level, transient rates will be underestimated by the factor  $\beta/(f + \beta)$ . At low levels of activation force ( $f \ll 1$ ) kinetics would be little affected by filament compliance ( $K_{\text{myo}} \gg K_X$ ), whereas at maximum force ( $f = 1$ ) the rate would be underestimated by the factor  $\beta/(1 + \beta)$ . Therefore, at maximum force,  $k^-$  in Fig. 5 is

underestimated by  $\sim 70\%$  ( $(1 - 0.43/1.43) \times 100$ ). Furthermore, Eq. 2 also indicates that the underestimation of rate does not depend on the absolute value of the rate of transient tension change being measured. Thus, if correction for a distribution of  $C_S$  between cross-bridges and myofilaments is not made, the rates of tension transients may be underestimated by the factor  $\beta/(f + \beta)$ , with the distortion increasing as maximum force is approached.

### SUMMARY

In actively contracting skinned rabbit skeletal fibers we found that  $C_S$ ,  $Y_0$ , and the rate of phase 2 tension redevelopment ( $r$ ) were all dependent on the level of  $\text{Ca}^{2+}$  activation.  $C_S$  and  $r$  decreased, whereas  $Y_0$  increased, as the level of contractile activation and force increased. The results were similar when force was altered by varying  $[\text{Ca}^{2+}]$ , inhibition with  $\text{AlF}_4^-$  at high  $[\text{Ca}^{2+}]$ , or without  $\text{Ca}^{2+}$  by reconstitution of thin filaments with aTnC. Fitting these results with a simple three-component series model of sarcomeric compliance resulted in an estimation of the fraction of total compliance due to myofilaments that was comparable to more direct measurements of filament compliance in isolated thin filaments and in activated intact muscles. Thus, the previous descriptions of activation-dependent cross-bridge kinetics and  $Y_0$  could be explained in large part by the presence of a substantial non-cross-bridge component of  $C_S$ .

We acknowledge Carol Freitag, Martha Mathiason, and Anthony Rivera for expert technical assistance and the National Institutes of Health for support (grants HL-51277, HL-52558, and HL 61683).

### REFERENCES

- Allen, T. S., N. Ling, M. Irving, and Y. E. Goldman. 1996. Orientation changes in myosin regulatory light chains following photorelease of ATP in skinned muscle fibers. *Biophys. J.* 70:1847–1862.
- Bagni, M. A., G. Cecchi, B. Colombini, and F. Colomo. 1999. Sarcomere tension-stiffness relation during the tetanus rise in single frog muscle fibers. *J. Muscle Res. Cell Motil.* 20:469–476.
- Bagni, M. A., G. Cecchi, F. Colomo, and C. Poggese. 1990. Tension and stiffness of frog muscle fibers at full filament overlap. *J. Muscle Res. Cell Motil.* 11:371–377.
- Bagni, M. A., G. Cecchi, and M. Schoenberg. 1988. A model of force production that explains the lag between cross-bridge attachment and force after electrical stimulation of striated muscle fibers. *Biophys. J.* 54:1105–1114.
- Brenner, B. 1983. Technique for stabilizing the striation pattern in maximally calcium-activated skinned rabbit psoas fibers. *Biophys. J.* 41:99–102.
- Chase, P. B., and M. J. Kushmerick. 1988. Effects of pH on contraction of rabbit fast and slow skeletal muscle fibers. *Biophys. J.* 53:935–946.
- Chase, P. B., D. A. Martyn, and J. D. Hannon. 1994. Activation dependence and kinetics of force and stiffness inhibition by aluminofluoride, a slowly dissociating analogue of inorganic phosphate, in chemically skinned fibers from rabbit psoas muscle. *J. Muscle Res. Cell Motil.* 15:119–129.

- Chase, P. B., D. A. Martyn, M. J. Kushmerick, and A. M. Gordon. 1993. Effects of inorganic phosphate analogues on stiffness and unloaded shortening of skinned muscle fibers from rabbit. *J. Physiol. (Lond.)* 460:231–246.
- Corrie, J. E. T., B. D. Brandmeier, R. E. Ferguson, D. R. Trentham, J. Kendrick-Jones, S. C. Hopkins, U. A. van der Heide, Y. E. Goldman, C. Sabido-David, R. E. Dale, S. Criddle, and M. Irving. 1999. Dynamic measurements of myosin-light-chain-domain tilt and twist in muscle contraction. *Nature* 400:425–430.
- Daniel, T. L., A. C. Trimble, and P. B. Chase. 1998. Compliant realignment of binding sites in muscle: transient behavior and mechanical tuning. *Biophys. J.* 74:1611–1621.
- Dantzig, J. A., Y. E. Goldman, N. C. Millar, J. Lacktis, and E. Homsher. 1992. Reversal of the cross-bridge force-generating transition by photogeneration of phosphate in rabbit psoas muscle fibers. *J. Physiol.* 451:247–278.
- Davis, J. S., and M. E. Rodgers. 1995. Force generation and temperature-jump and length-jump tension transients in muscle fibers. *Biophys. J.* 68:2032–2040.
- Ford, L. E., A. F. Huxley, and R. M. Simmons. 1977. Tension responses to sudden length change in stimulated frog muscle fibers near slack length. *J. Physiol.* 269:441–515.
- Ford, L. E., A. F. Huxley, and R. M. Simmons. 1981. The relation between stiffness and filament overlap in stimulated frog muscle fibers. *J. Physiol.* 311:219–249.
- Ford, L. E., A. F. Huxley, and R. M. Simmons. 1986. Tension transients during the rise of tetanic tension in frog muscle fibers. *J. Physiol.* 372:595–609.
- Geeves, M. A., and S. S. Lehrer. 1994. Dynamics of the muscle thin filament regulatory switch: the size of the cooperative unit. *Biophys. J.* 67:273–282.
- Gordon, A. M., E. Homsher, and M. Regnier. 2000. Regulation of contraction in striated muscle. *Physiol. Rev.* 80:853–924.
- Gordon, A. M., A. F. Huxley, and F. J. Julian. 1966. The variation in isometric tension with sarcomere length in vertebrate muscle fibers. *J. Physiol.* 184:170–192.
- Hannon, J. D., P. B. Chase, D. A. Martyn, L. L. Huntsman, M. J. Kushmerick, and A. M. Gordon. 1993. Calcium-independent activation of skeletal muscle fibers by a modified form of cardiac troponin C. *Biophys. J.* 64:1632–1637.
- Higuchi, H., T. Yanagida, and Y. E. Goldman. 1995. Compliance of thin filaments in skinned fibers of rabbit skeletal muscle. *Biophys. J.* 69:1000–1010.
- Howard, J. 1997. Molecular motors: structural adaptations to cellular functions. *Nature* 389:561–567.
- Huxley, A. F., and R. M. Simmons. 1971. Proposed mechanism of force generation in striated muscle. *Nature* 233:533–538.
- Huxley, A. F., and R. M. Simmons. 1972. Mechanical transients and the origin of muscular force. *Cold Spring Harbor Symp. Quant. Biol.* 37:669–680.
- Huxley, H. E., A. Stewart, H. Sosa, and T. Irving. 1994. X-ray diffraction measurements of the extensibility of actin and myosin filaments in contracting muscle. *Biophys. J.* 67:2411–2421.
- Isambert, H., P. Venier, A. C. Maggs, A. Fattoum, R. Kassab, D. Pantaloni, and M.-F. Carlier. 1995. Flexibility of actin filaments derived from thermal fluctuations: effect of bound nucleotide, phalloidin, and muscle regulatory proteins. *J. Biol. Chem.* 270:11437–11444.
- Kawai, M., R. N. Cox, and P. W. Brandt. 1981. Effect of Ca ion concentration on cross-bridge kinetics in rabbit psoas fibers: evidence for the presence of two Ca-activated states of thin filament. *Biophys. J.* 35:375–384.
- Kojima, H., A. Ishijima, and T. Yanagida. 1994. Direct measurement of stiffness of single actin filaments with and without tropomyosin by in vitro nanomanipulation. *Proc. Natl. Acad. Sci. U.S.A.* 91:12962–12966.
- Linari, M., I. Dobbie, M. Reconditi, N. Koubassova, M. Irving, G. Piazzesi, and V. Lombardi. 1998. The stiffness of skeletal muscle in isometric contraction and rigor: the fraction of heads bound to actin. *Biophys. J.* 74:2459–2473.
- Linari, M., G. Piazzesi, and V. Lombardi. 2002. Effects of *N*-benzyl-*P*-toluene sulfonamide (BTS) on force and stiffness of active single fibers of frog skeletal muscle. *Biophys. J.* 82:377a. (Abstr.)
- Luo, Y., R. Cooke, and E. Pate. 1994. Effect of series elasticity on delay in development of tension relative to stiffness during muscle activation. *Am. J. Physiol.* 267:C1598–C1606.
- Malloy, J. E., J. E. Burns, J. Kendrick-Jones, R. T. Tregear, and D. C. S. White. 1995. Movement and force produced by a single myosin head. *Nature* 378:209–212.
- Martyn, D. A., and P. B. Chase. 1995. Faster force transient kinetics at submaximal  $\text{Ca}^{2+}$  activation of skinned psoas fibers from rabbit. *Biophys. J.* 68:235–242.
- Martyn, D. A., and A. M. Gordon. 1992. Force and stiffness in glycerinated rabbit psoas fibers: effects of calcium and elevated phosphate. *J. Gen. Physiol.* 99:795–816.
- Matsubara, I., Y. Umazume, and N. Yagi. 1985. Lateral filamentary spacing in chemically skinned murine muscles during contraction. *J. Physiol.* 360:135–148.
- McKillop, D. F. A., and M. A. Geeves. 1993. Regulation of the interaction between actin and myosin subfragment 1: evidence for three states of the thin filament. *Biophys. J.* 65:693–701.
- Mijailovich, S. M., J. Fredberg, and J. P. Butler. 1996. On the theory of muscle contraction: filament extensibility and the development of isometric force and stiffness. *Biophys. J.* 71:1475–1484.
- Piazzesi, G., F. Francini, M. Linari, and V. Lombardi. 1992. Tension transients during steady lengthening of tetanized muscle fibers of the frog. *J. Physiol.* 445:659–711.
- Putkey, J. A., D. G. Dotson, and P. Mouawad. 1993. Formation of inter- and intramolecular disulfide bonds can activate cardiac troponin C. *J. Biol. Chem.* 268:6827–6830.
- Ranatunga, K. W. 1996. Endothermic force generation in fast and slow mammalian (rabbit) muscle fibers. *Biophys. J.* 71:1905–1913.
- Regnier, M., C. Morris, and E. Homsher. 1995. Regulation of the cross-bridge transition from a weakly to strongly bound state in skinned rabbit muscle fibers. *Am. J. Physiol.* 269:C1532–C1539.
- Smith, C. A., and I. Rayment. 1995. X-ray structure of the magnesium(II)-ADP-vanadate complex of the *Dictyostelium discoideum* myosin motor domain to 1.9 Å resolution. *Biochemistry* 35:5404–5417.
- Swartz, D. R., R. L. Moss, and M. L. Greaser. 1996. Calcium alone does not fully activate the thin filament for S1 binding to rigor myofibrils. *Biophys. J.* 71:1891–1904.
- Tawada, K., and M. Kimura. 1984. Stiffness of glycerinated rabbit psoas fibers in the rigor state: filament-overlap relation. *Biophys. J.* 45:593–602.
- Wakabayashi, K., Y. Sugimoto, H. Tanaka, Y. Ueno, Y. Takezawa, and Y. Amemiya. 1994. X-ray diffraction evidence for the extensibility of actin and myosin filaments during muscle contraction. *Biophys. J.* 67:2422–2435.